Author(s): Koivistoinen, Juha; Aumanen, Jukka; Hiltunen, Vesa-Matti; Myllyperkiö, Pasi; Johansson, Andreas; Pettersson, Mika

Title: Real-time monitoring of graphene patterning with wide-field four-wave mixing microscopy

Year: 2016

Version:

Please cite the original version:

Koivistoinen, J., Aumanen, J., Hiltunen, V.-M., Myllyperkiö, P., Johansson, A., & Pettersson, M. (2016). Real-time monitoring of graphene patterning with wide-field four-wave mixing microscopy. Applied Physics Letters, 108(15), Article 153112. https://doi.org/10.1063/1.4946854

AIP | Applied Physics Letters

Real-time monitoring of graphene patterning with wide-field four-wave mixing microscopy

Juha Koivistoinen, Jukka Aumanen, Vesa-Matti Hiltunen, Pasi Myllyperkiö, Andreas Johansson, and Mika Pettersson

Citation: Applied Physics Letters **108**, 153112 (2016); doi: 10.1063/1.4946854
View online: http://dx.doi.org/10.1063/1.4946854
View Table of Contents: http://scitation.aip.org/content/aip/journal/apl/108/15?ver=pdfcov
Published by the AIP Publishing

Real-time monitoring of graphene patterning with wide-field four-wave mixing microscopy

Juha Koivistoinen,[1] Jukka Aumanen,[1] Vesa-Matti Hiltunen,[2] Pasi Myllyperkiö,[1] Andreas Johansson,[1,2] and Mika Pettersson[1,a)]
[1]*Department of Chemistry, Nanoscience Center, University of Jyväskylä, P.O. Box 35, Jyväskylä FI-40014, Finland*
[2]*Department of Physics, Nanoscience Center, University of Jyväskylä, P.O. Box 35, Jyväskylä FI-40014, Finland*

(Received 26 January 2016; accepted 26 March 2016; published online 15 April 2016)

The single atom thick two-dimensional graphene is a promising material for various applications due to its extraordinary electronic, optical, optoelectronic, and mechanical properties. The demand for developing graphene based applications has entailed a requirement for development of methods for fast imaging techniques for graphene. Here, we demonstrate imaging of graphene with femtosecond wide-field four-wave mixing microscopy. The method provides a sensitive, non-destructive approach for rapid large area characterization of graphene. We show that the method is suitable for online following of a laser patterning process of microscale structures on single-layer graphene. *Published by AIP Publishing*. [http://dx.doi.org/10.1063/1.4946854]

Properties of nano-objects with varying size and atomic level structure have been investigated in hopes to find candidates for technological applications, such as photodetectors,[1] optical modulators,[2] photovoltaic cells,[3] and nanoelectronics.[4] Graphene, composed solely of carbon which is one of the most abundant elements on earth, bears all of the properties required for harnessing it for the above-mentioned applications.[5–8]

Whereas many standard techniques, such as optical microscopy, atomic force microscopy (AFM), scanning electron microscopy (SEM), transmission electron microscopy (TEM), and scanning tunneling microscopy (STM), may be used for imaging of graphene, they are unable to rapidly scan large areas with high sensitivity. Most of these methods are time-consuming, require substrate or extra sample preparation steps or vacuum conditions, or ultimately cause damage to the sample.

Raman spectroscopy is possibly the most commonly used method for characterization of graphene, due to the strong signal and characteristic and informative spectrum, and fairly easy access to the technique.[9,10] Despite the advantages of Raman imaging, it is a relatively slow imaging technique and the high laser power required for faster imaging may cause damage to the sample.

Graphene has an exceptionally large third order susceptibility ($\chi^{(3)} \sim 10^{-7}$ esu), and third order non-linear methods, such as Four-Wave Mixing (FWM) imaging, have been found feasible for the characterization of graphene[11,12] similarly to other related carbon nanomaterials, such as carbon nanotubes.[13–15] Recently, rapid imaging of large areas of graphene by scanning mode FWM was demonstrated.[16] Also, other non-linear methods, such as third harmonic generation (THG) and multiphoton absorption excited fluorescence (MAEF), have been shown to be capable for rapid large area imaging of graphene.[17]

FWM is a sensitive technique and it offers many variants for exploiting either electronic or vibrational properties for imaging of various materials.[18] In wide-field FWM imaging, short laser pulses are used to generate the FWM signal in the sample. Large area is illuminated using conventional lens, and the signal is collected with microscope objective, exploiting the generated FWM signal as an internal light source. Wide field geometry allows single-shot imaging which opens interesting possibilities for visualization of dynamical processes. This is not possible with an alternative approach which involves constructing the image by scanning the sample by multiple point-by-point measurements with tight focusing using a microscope objective. This approach yields better resolution than wide field method due to non-linear signal generation, but for one atom-thick material, this concerns only lateral dimension. Wide field FWM imaging can be performed with common amplified femtosecond laser systems, and it does not require more complicated setup compared to the scanning mode FWM imaging which is more commonly used. The first wide-field CARS microscope based on picosecond laser pulses was reported by Reintjes *et al*. as early as 1982.[19] More recently, wide-field FWM and its variants have been applied for non-linear optical imaging of nanostructures and molecular systems but not for graphene so far.[18,20,21]

Recently, optical patterning of graphene via two-photon oxidation, using femtosecond pulses, was reported.[12] Subsequently, oxidation patterning of graphene was reported to succeed also with picosecond pulses.[22] The photo-oxidation process enables controllable tuning of the electronic properties of graphene, including opening of a band gap.[12] The driving force for the development of the wide-field FWM microscope, presented in this research, was imaging of oxidized patterns with FWM imaging, which was previously carried out in a scanning mode.[12] For further development of the patterning technique, rapid online monitoring of the process is needed. The development of such a technique was the original motivation of the present work.

Here, we present fast, non-destructive, large area, femtosecond wide-field FWM imaging method for graphene. Online following of oxidation patterning of single layer

a)Author to whom correspondence should be addressed. Electronic mail: mika.j.pettersson@jyu.fi

graphene (SLG) is demonstrated as an example of process monitoring. We use three separate femtosecond beams with different wavelengths that provide flexibility for tuning Stokes shift and signal wavelength, and yield optimal conditions for spectral filtering of the FWM signal. The setup and the experimental parameters are fully described in supplementary material (see supplementary material, Fig. S1).[23]

All the measurements were performed on air-suspended SLG, which was obtained from a commercial vendor (Graphene Platform) and its quality was verified with Raman spectroscopy (see supplementary material, Fig. S2).[23] SLG was supported on a copper TEM grid with $7 \times 7\ \mu m^2$ holes (see supplementary material, Fig. S3).[23] The fundamental beam ($\lambda = 800$ nm; R = 1 kHz; $E_{pulse} = 1$ mJ) was split in three, each modified using non-collinear optical parametric amplification (NOPA) and pulse compression with prisms, yielding <55 fs pulses and wavelengths of 610, 670, and 585 nm corresponding to pump, Stokes, and probe, respectively (Fig. S1B). The beams were recombined at the sample by applying BOXCARS geometry, simultaneously fulfilling spatial and temporal overlap and phase-matching conditions,[24] producing a 538 nm FWM signal. However, it should be noted that phase-matching is not necessary for an atomic-thin sample. Pulse energy for imaging was 35 nJ for each beam, corresponding to peak intensity of 3.2×10^{10} W/cm^2. At these intensities, photo-oxidation was avoided as it occurs with high efficiency only for intensities exceeding 10^{11} W/cm^2.[12]

Before starting the measurements, the signal was confirmed as a FWM signal, first by observing total loss of the signal while blocking each beam separately, and second, by gradually observing loss of the signal intensity while moving the probe delay stage away from the maximum temporal overlap position (see supplementary material, Fig. S1C).[23] Furthermore, transmission of scattered illumination light was ruled out as a source of image contrast by comparing an optical image, obtained with white light illumination with a wide-field FWM image. In the FWM image, the signal was observed, with high contrast, solely from the locations where the material was present, while in the white light, optical image signal was observed in all the transparent parts of the sample. Consequently, it can be claimed with confidence that the observed signal originates from the FWM process. Some minor leakage from the spectral tail of the probe beam and the residuals from the white light continuum of NOPA of the pump beam were observed, but these were effectively subtracted when removing the background noise.

The wide-field FWM imaging was studied using SLG, patterned with oxidized structures by the two-photon oxidation method described earlier.[12] In brief, a tightly focused femtosecond laser beam was used to oxidize graphene locally. Oxidation reduces the FWM response of graphene close to zero, providing a contrast mechanism for imaging. Various patterns were drawn by computer-controlled movement of the oxidation beam. An EMCCD camera (Andor Newton) was used for image recording.

A FWM image and an optical image of the sample are shown in Figs. 1(a) and 1(b), respectively. The signal intensity is not uniform over the exposed area due to the Gaussian beam profile, and additionally, the shape of the illuminated spot is not perfectly round but it is flattened in the vertical direction. The useful imaging area for single exposure is approximately $80 \times 50\ \mu m^2$. Several $7 \times 7\ \mu m^2$ windows covered with air-suspended and patterned SLG are visible in the wide-field FWM image (Fig. 1(a)). The FWM signal varies owing to the oxidation patterns and inhomogeneities (ripples, folds, grain boundaries, or impurities), the former manifested as dark areas and the latter as brighter spots. The typical non-patterned SLG on an opening can be seen greyish in Fig. 1(a), and the dark areas between the windows correspond to the copper grid which blocks any FWM signal in the applied measurement geometry. Moreover, the window openings producing no signal are not covered with graphene.

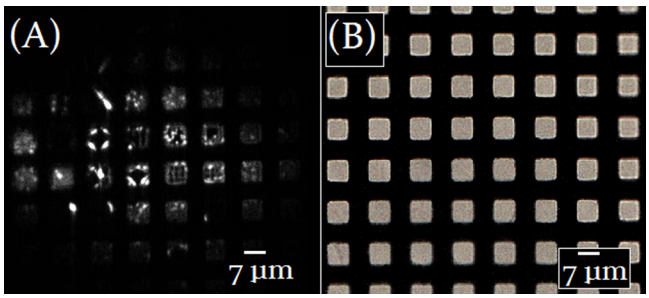

FIG. 1. (a) FWM image of a TEM copper grid with $7 \times 7\ \mu m^2$ openings covered with patterned suspended single layer graphene. The patterned features as well as the windows with no graphene produce no signal, unlike in the optical image (b) where the light is transmitted nearly uniformly through all the windows.

For comparison, in Fig. 1(b), a white light transmission image of the same area is shown, demonstrating that it is not possible to distinguish the patterned features or the inhomogeneities from the linear optical image. Furthermore, it is not possible to see if an opening is covered with graphene or not, whereas the FWM image shows excellent contrast in both cases.

The accumulation time for the wide-field image, presented in Fig. 1(a), was 10 s, and with this collection time, the maximum intensity from SLG graphene (not from bright spots) exceeded 10 000 counts/pixel. This relatively long acquisition time was used for obtaining high intensity signal and sharp contrast in order to well resolve even the small features, but it is clear that based on the high signal level, much faster imaging could be performed. For imaging larger features, one could easily use ten times shorter integration time. If necessary, it would also be possible to speed acquisition by increasing laser pulse energy or repetition rate.

A comparison between wide-field and scanning mode FWM images of several individual windows of the sample is shown in Figs. 2(a) and 2(b), respectively. The corresponding oxidation patterns are clearly present in both figures, along with other features that are due to various inhomogeneities. Cross sections of the corresponding areas are shown on the right, emphasizing the high signal and contrast. The resolution in the scanning mode image (Fig. 2(b)) is slightly better than in the wide-field image (Fig. 2(a)) due to the nonlinear excitation process, but otherwise they correspond well with each other.

The experimental resolution in the wide field images is approximately 1 μm as can be judged from the narrow feature in the cross-section. This is somewhat worse than the

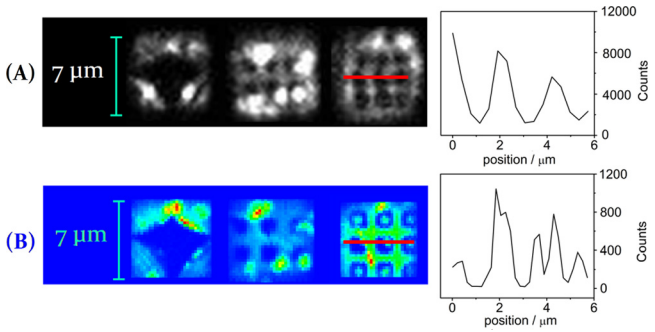

FIG. 2. FWM images of the patterned SLG windows imaged in (a) wide-field geometry with a 1 kHz laser and (b) point-by-point scanning mode with a 600 kHz laser. Intensity cross sections measured along the red lines are shown on the right. Note the different scales of the y-axis in the figures.

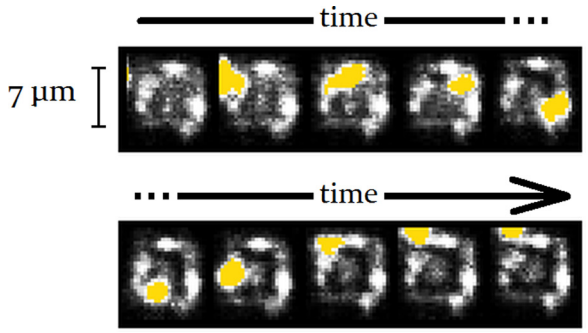

FIG. 3. Series of snapshots from the online photo-oxidation video of a graphene-covered opening. The yellow spot is the oxidation beam, having an intensity of 7.7×10^{11} W/cm^2. The photo-oxidation produces changes that appear as dark areas in the FWM image. (Multimedia view) [URL: http://dx.doi.org/10.1063/1.4946854.1]

diffraction limited resolution of $\sim 0.5\,\mu$m expected for the microscope objective with NA = 0.55 and for the central wavelength of the signal at 538 nm. The discrepancy can be explained by experimental factors such as imperfect optics and alignment. The detector pixel size ($16 \times 16\,\mu$m^2) is not a limiting factor for the resolution here, since the area of one pixel corresponds to the sample area of $0.32 \times 0.32\,\mu$m^2 allowing ~ 2 pixels per diffraction limited spot diameter which should be sufficient. Further improvements in resolution can be obtained by using higher NA objectives and better optical alignment.

For the presented method, it is interesting to estimate the prospects for even larger area imaging considering the possibilities of currently available technology. As the pulse energy required to generate the FWM signal is very small, potentially very large areas can be irradiated with available laser sources. Reasonable peak intensity for imaging is 5×10^{10} W/cm^2, corresponding to a pulse energy density of 3 mJ/cm^2, with 60 fs pulses. MilliJoule-level pulse energies are easily available in common amplified femtosecond laser systems, but since wavelength tuning is required, it is reasonable to assume an output of up to 10 μJ/cm^2 from high level NOPAs. Accordingly, areas close to 1 mm^2 could be imaged possibly with video rate speed, using suitable objectives and cameras. Thus, the present method is very promising for large-area online characterization of graphene.

We used FWM wide-field imaging for online monitoring of patterning of graphene with two-photon oxidation. A tightly focused femtosecond laser beam ($\lambda = 590$ nm) from a high repetition rate laser setup (600 kHz) was directed to the sample from the backside, with respect to the direction of FWM imaging, using an additional 45° dichroic long-pass filter (see supplementary material, Fig S1D),[23] in order to write patterns on suspended SLG while simultaneously monitoring the process by FWM wide-field imaging in video mode. The oxidation beam was manually moved over the sample by adjusting the mirror guiding the beam to the aperture of the microscope objective. The maximum intensity of the oxidation beam at the sample was estimated to be $\sim 1.0 \times 10^{12}$ W/cm^2, which was then tuned with a neutral density filter.

In Fig. 3 (multimedia view), snapshots from the online oxidation experiment are shown. In each individual frame, a bright yellow spot shows the current position of the oxidation beam. The brighter white areas are inhomogeneities giving locally higher signal. As the incident oxidation beam, with intensity of 7.7×10^{11} W/cm^2, moved through the graphene window, it induced photo-oxidation of the exposed area with the resulting decrease of the intensity of the FWM signal, which can be seen forming a closed square shaped pattern.[12]

The data in Fig. 3 and the video in supporting data show that wide-field FWM imaging can be used for the following processes, such as optically induced photo-oxidation performed on graphene, in real-time. In the previous investigations, patterning of graphene by photo-oxidation or laser induced thinning of graphene was followed by sequential patterning and FWM imaging.[12,16] Here, we make a step toward more advanced control of optical processing of graphene by performing processing and imaging simultaneously. A possible additional application of the presented technique is following the growth of graphene single crystals *in situ* in real-time.

In conclusion, we have presented a femtosecond wide-field FWM imaging method for online monitoring of two-photon oxidation of graphene. Video mode imaging was demonstrated, indicating strong signal levels and high imaging speed, which can be exploited for fast imaging of large areas. This demonstrates a possibility for real-time control of patterning or other processing of graphene as well as monitoring the growth of graphene.

This work was funded by the Academy of Finland (Decision No. 252468).

[1]L. Hu, L. Wu, M. Liao, and X. Fang, Adv. Mater. **23**, 1988 (2011).
[2]G. T. Reed, G. Mashanovich, F. Y. Gardes, and D. J. Thomson, Nat. Photonics **4**, 518 (2010).
[3]S. Chang, Q. Li, X. Xiao, K. Y. Wong, and T. Chen, Energy Environ. Sci. **5**, 9444 (2012).
[4]A. Taraso, P. M. Campbell, M.-Y. Tsai, Z. R. Hesabi, J. Feirer, W. J. Graham, S. Ready, and E. M. Vogel, Adv. Funct. Mater. **24**, 6389 (2014).
[5]P. Avouris, Z. Chen, and V. Perebeinos, Nat. Nanotechnol. **2**, 605 (2007).
[6]J. Li, L. Niu, Z. Zheng, and F. Yan, Adv. Mater. **26**, 5239 (2014).
[7]M. Liu, X. Yin, E. Ulin-Avila, B. Geng, T. Zentgraf, L. Ju, F. Wang, and X. A. Zhang, Nature **474**, 64 (2011).
[8]F. Withers, T. H. Bointon, M. F. Craciun, and S. Russo, ACS Nano **7**, 5052 (2013).
[9]A. C. Ferrari, J. C. Meyer, V. Scardaci, C. Casiraghi, M. Lazzeri, F. Mauri, S. Piscanec, D. Jiang, K. S. Novoselov, S. Roth *et al.*, Phys. Rev. Lett. **97**, 187401 (2006).
[10]R. W. Havener, S.-Y. Ju, L. Brown, Z. Wang, M. Wojcik, C. S. Ruiz-Vargas, and J. Park, ACS Nano **6**, 373 (2012).

[11]E. Hendry, P. J. Hale, J. Moger, A. K. Savchenko, and S. A. Mikhailov, Phys. Rev. Lett. **105**, 097401 (2010).
[12]J. Aumanen, A. Johansson, J. Koivistoinen, P. Myllyperkiö, and M. Pettersson, Nanoscale **7**, 2851 (2015).
[13]P. Myllyperkiö, O. Herranen, J. Rintala, H. Jiang, P. R. Mudimela, Z. Zhu, A. G. Nasibulin, A. Johansson, E. I. Kauppinen, M. Ahlskog *et al.*, ACS Nano **4**, 6780 (2010).
[14]H. Kim, T. Sheps, P. G. Collins, and E. O. Potma, Nano Lett. **9**, 2991 (2009).
[15]J. Aumanen, A. Johansson, O. Herranen, P. Myllyperkiö, and M. Pettersson, Phys. Chem. Chem. Phys. **17**, 209 (2015).
[16]D. W. Li, Y. S. Zhou, X. Huang, L. Jiang, J.-F. Silvain, and Y. F. Lu, Nanoscale **7**, 3651 (2015).
[17]A. Säynätjoki, L. Karvonen, J. Riikonen, W. Kim, S. Mehravar, R. A. Norwood, N. Peyghambarian, H. Lipsanen, and K. Kieu, ACS Nano **7**, 8441 (2013).
[18]Y. Wang, X. Liu, A. R. Halpern, K. Cho, R. M. Corn, and E. O. Potma, Appl. Opt. **51**, 3305 (2012).
[19]J. Reintjes, M. D. Duncan, and T. J. Manuccia, Proc. SPIE **322**, 87 (1982).
[20]C. Heinrich, S. Bernet, and M. Ritsch-Marte, Appl. Phys. Lett. **84**, 816 (2004).
[21]M. Lei, M. Winterhalder, R. Selm, and A. Zumbusch, J. Biomed. Opt. **16**, 021102 (2011).
[22]I. I. Bobrinetskiy, N. Emelianov, N. Otero, and P. M. Romero, Appl. Phys. Lett. **107**, 043104 (2015).
[23]See supplementary material at http://dx.doi.org/10.1063/1.4946854 for the description of the experimental setup and methods, Raman spectrum of graphene and description of the samples.
[24]D. Romanov, A. Filin, R. Compton, and R. Levis, Opt. Lett. **32**, 3161 (2007).